

Universal properties of violently relaxed gravitational structures

Francesco Sylos Labini^{1,2}

¹*Centro Studi e Ricerche Enrico Fermi, Via Panisperna 00184 - Rome - Italy*

²*Istituto dei sistemi complessi, Consiglio Nazionale delle Ricerche, Via dei Taurini 19, 00185 Rome, Italy*

17 October 2018

ABSTRACT

We study the collapse and virialization of an isolated spherical cloud of self-gravitating particles initially at rest and characterised by a power-law density profile, with exponent $0 \leq \alpha < 3$, or by a Plummer, an Hernquist, a NFW, a Gaussian profile. We find that in all cases the virialized structure formed after the collapse has a density profile decaying, at large enough radii, as $\sim r^{-4}$, and a radial velocity dispersion profile decaying as $\sim r^{-1}$. We show that these profiles originate from the physical mechanism responsible of the ejection of a fraction of cloud’s mass and energy during the collapse and that this same mechanism washes out the dependence on the initial conditions. When a large enough initial velocity dispersion is given to the cloud particles, ejection does not occur anymore and consequently the virialized halo density and velocity profiles display features which reflect the initial conditions.

Key words: Galaxy: halo; Galaxy: formation; globular clusters: general; (cosmology:) dark matter; (cosmology:) large-scale structure of Universe; galaxies: formation

1 INTRODUCTION

It is well known that some of the properties of virialized structures formed through the gravitational collapse of an isolated system depend on the initial conditions in various ways; however, some other statistical features of these structures seem to be generated by the dynamical mechanisms acting during the relaxation process (see e.g., van Albada (1982); Aarseth et al. (1988); Theis & Spurzem (1999); Boily & Athanassoula (2006); Joyce, Marcos & Sylos Labini (2009a,b); Visbal, Loeb & Hernquist (2012) and references therein).

For instance, when a spatially uniform and isolated cloud of density ρ_0 and with a small enough initial velocity dispersion collapses, it forms, in a time-scale $\tau_D = \sqrt{3\pi/(32G\rho_0)}$, a virialized structure characterised, for radii larger than the size of a dense inner core r_c , by (i) a power-law density profile $n(r) \sim r^{-4}$, (ii) a radial velocity dispersion which decays in a Keplerian way $\sigma_r^2(r) \sim r^{-1}$ and (iii) a pseudo phase-space density that decays as $n(r)/\sigma_r^3(r) \sim r^{-5/2}$ (Sylos Labini 2012).

These behaviors were shown to be associated with the ejection of a fraction of the initial mass and energy from the system during the collapse: in particular, particles with binding energies close to zero follows almost radial orbits around the dense core, thus displaying a Keplerian velocity dispersion. Considering that they conserve their total energy it is possible to show that the density profile fol-

lows the observed $n(r) \sim r^{-4}$ decay (Sylos Labini 2012). Note that the crucial role of particles ejection for the formation of non-trivial density and velocity profiles has not been properly appreciated in the literature (see discussion in Joyce, Marcos & Sylos Labini (2009a); Sylos Labini (2012)).

In order to study whether the behaviors (i)-(iii) above are found in the collapse of spherical clouds with different initial density profiles than uniform and to determine whether in more general cases there remains memory of the initial conditions after the collapse phase, we consider (i) a set of clouds with an initial density profile of the type $n(r) = n_\alpha/r^\alpha$, where n_α is a constant and $0 \leq \alpha < 3$ and (ii) density profiles without a simple scale free behaviour, e.g., a Plummer sphere, an Hernquist profile (Hernquist 1990), a Navarro Frenk and White (NFW) profile (Navarro, Frenk & White 1997) and a Gaussian profile.

Note that while the formation and evolution of self-gravitating dissipation-less systems is a theoretical interesting and complex problem, the simple models considered here may only help to develop tools and analysis to understand more realistic systems for which it is then necessary to consider the role of merging, of dissipation and the fact that they cannot be simply considered isolated. Whether these complications qualitatively change the evolution with respect to the simple systems considered here will be studied in a forthcoming publication. However, the collapse of

an isolated cloud of self-gravitating particles may describe the formation of elliptical galaxies (Hénon 1964; van Albada 1982; Sylos Labini 2012) which are characterised by the de Vaucouleurs $R^{1/4}$ law. A possible analytical approximation to the de-projected $R^{1/4}$ is given by the Hernquist profile (Hernquist 1990; Visbal, Loeb & Hernquist 2012) which is indeed characterised by a r^{-4} decay at large radii.

The paper is organised as follows. We present in Sect.2 the details of the numerical simulations that we have performed. The case of an initially scale free profile is discussed in Sect.3. We then consider in Sect.4 more complex density profiles, which have a characteristic length. Finally in Sect.5 we discuss the results draw our main conclusions.

2 THE SIMULATIONS

The initial conditions are generated by distributing N particles randomly with density $n(r)$, where r is the distance from the origin of coordinates. For the scale free density profiles $n(r) = n_\alpha r^{-\alpha}$, where $0 \leq \alpha < 3$: for larger values of α and $r \rightarrow 0$ there are too many nearest neighbours with arbitrarily small distance. In such a situation an accurate numerical integration of the equations of motion becomes very problematic. We put a lower and an upper cut-off: the latter is of the order of the softening length of the code and the former, R_0 , is larger than any characteristic scale of the profile (if present).

We generate a series of spherical clouds of particles, with $N = 10^4$ and with different initial virial ratio $b_0 = b(t=0) = 2K_0/W_0$ (where K/W is the kinetic/potential energy). In order to assign velocities we take the velocity components to have a uniform probability density function (PDF) in the range $[-V_0, V_0]$ so that the modulus of the velocity is constrained to be in a sphere of radius V_0 . The velocity PDF is thus

$$g(v) = \frac{3}{V_0^3} v^2 \text{ for } v \leq V_0 \quad (1)$$

and zero otherwise. The mean square value of the velocity is

$$\langle v^2 \rangle = \int_0^{V_0} v^2 g(v) dv = \frac{3}{5} V_0^2 = \frac{W_0 b_0}{mN}. \quad (2)$$

We used the publicly available tree-code GADGET (Springel et al. 2001; Springel 2005) to run the simulations. We have chosen the same combination of numerical parameters as in Sylos Labini (2012), to which we refer the reader for further details on the numerical issues.

3 SCALE-FREE PROFILES

We first discuss the relaxation of a spherical and isolated cloud, with a with a power-law profile, initially at rest. Then we consider the effect of a non-zero initial velocity dispersion.

3.1 Virial ratio

The virial ratio for all system particles $b_a(t)$ and the virial ratio for bound $b_n(t)$ have a different amplitude (see upper left and right panels of Fig.1): this can be easily explained as

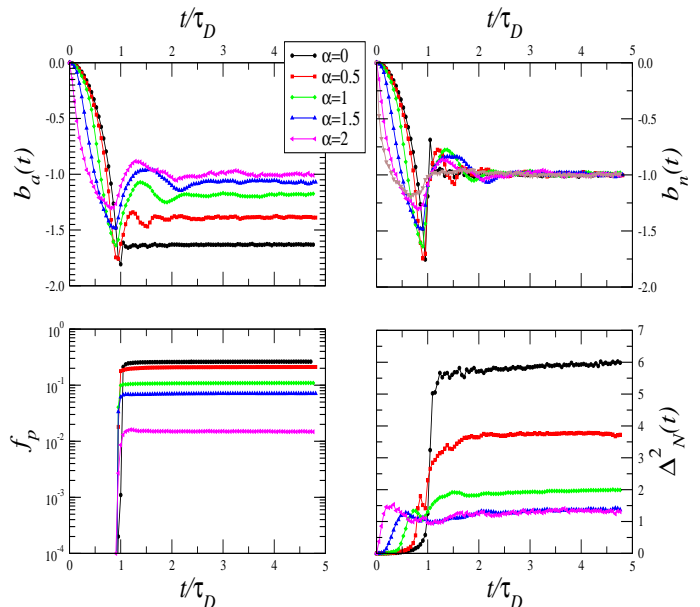


Figure 1. Upper left panel: Virial ratio of all particles. Upper right panel: Virial ratio of particles with negative total energy. Bottom left panel: Fraction of particles with positive energy. Bottom right panel: Behaviors of the (normalised) energy exchanged $\Delta_N(t)$ (see text for details).

due to the fact that part of the particles have been ejected during the collapse. Indeed, the fraction of particles $f_p(t)$ with positive energy has an abrupt change becoming larger than zero for $t \geq \tau_D$ (see Fig.1 — bottom left panel). For $\alpha \geq 2$ only $f_p(t) \approx 1\%$ of the particles gain positive energy during the collapse while for $\alpha = 0$ we find $f_p(t) > 20\%$: the amount of ejected particles decreases with α and so the difference between $b_{tot}(t)$ and $b_{neg}(t)$.

3.2 Ejection

As discussed in detail in Joyce, Marcos & Sylos Labini (2009a); Sylos Labini (2012) the mechanism allowing particles to gain energy during the collapse phase arises from the interplay between the growth of density perturbations in the collapsing cloud and the finite size of the system. In practice, particles that were originally in the outer shells of the cloud arrive later than the others in the centre, thus moving, for a short time interval around τ_D , in a rapidly varying gravitational potential. As noticed above, even when $\alpha > 0$ some particles acquire positive energy at about $t \approx \tau_D$, i.e. when all other particles have already arrived to the centre and inverted their velocities. The difference between the case $\alpha = 0$ and $\alpha > 0$, and so the variation of f_p with α , is due to the different time of arrival at the centre of particles initially placed at different radii.

In the fluid limit and neglecting density perturbations, a particle initially placed at r_0 obeys to the following para-

metric equations:

$$r(\xi) = \frac{r_0}{2}(1 + \cos(\xi)) \quad (3)$$

$$t(\xi) = \sqrt{\frac{r_0^3}{8GM(r_0)}} (\xi + \sin(\xi)) ,$$

where

$$M(r_0) = \int_0^{r_0} mn_\alpha r^{-\alpha} 4\pi r^2 dr = \frac{4\pi}{3-\alpha} mn_\alpha r_0^{3-\alpha} . \quad (4)$$

Thus we get that a particle initially at r_0 arrives at the origin for $\xi = \pi$ and thus at

$$\tau(r_0; \alpha) = \sqrt{\frac{r_0^3 \pi^2}{8GM(r_0)}} = \sqrt{\frac{(3-\alpha)\pi r_0^\alpha}{32mn_\alpha G}} , \quad (5)$$

i.e., particles initially placed in the outer shells arrive later than the others for $\alpha > 0$ even if they follow their unperturbed trajectories. Instead, in this same limit, for $\alpha = 0$ all particles should arrive simultaneously at the centre, i.e., $\tau(r_0, 0) \equiv \tau_D \forall r_0$.

Noticing that for $r_0 = R_0$ we have $M(R_0) = mN$ and $\rho_0 = M(R_0)/V(R_0) = 3mN/(4\pi R_0^3)$ we find that

$$\tau(r_0 < R_0; \alpha) < \tau(R_0; \alpha) = \tau_D \quad \forall \alpha . \quad (6)$$

Thus the maximum time taken by a particle to arrive to the centre does not depend on α . Given that we detect particles with positive energy only for $t \geq \tau_D$, being τ_D the time taken by the particles in the outer shell to arrive at the centre, we may conjecture that, as it occurs for the $\alpha = 0$ case, ejected particles are those which initially lie in the outer shells: indeed Fig.2 (upper right panel) shows that this is the case.

In order to estimate the scaling of the fraction of ejected particles as a function of α , let us suppose that all ejected particles belong initially to the outer shell, i.e. they have at time $t = 0$ radius $r_0 \in [R_0 - \Delta R, R_0]$. The number of particles in this last shell scale as¹

$$\Delta N = \int_{R_0 - \Delta R}^{R_0} 4\pi n_\alpha r^{2-\alpha} dr = N \left(1 - \left(1 - \frac{\Delta R}{R_0} \right)^{3-\alpha} \right) \quad (7)$$

where we used the normalisation condition (N is fixed)

$$n_\alpha = \frac{(3-\alpha)N}{4\pi R_0^{3-\alpha}} . \quad (8)$$

The scaling behaviour of the fraction of ejected particles as a function of α derived from Eq.7, i.e. $f_p = \Delta N/N$, is shown in Fig.2 (upper left panel), together with the simulation points. (Note that the amplitude is fixed by the choice of ΔR .) One may see that a very rough agreement is found: in principle, one should use the true probability $p(r_0)$ for a particle to be ejected as a function of its initial radial position r_0 . For instance, by assuming $p(r_0) \sim r_0^\beta$ with $\beta > 3$, as measured in Joyce, Marcos & Sylos Labini (2009a) for the case $\alpha = 0$, we find

$$\frac{\Delta N}{N} \propto \frac{3-\alpha}{3-\alpha+\beta} . \quad (9)$$

¹ This corresponds to assuming a radial probability distribution for a particle initially placed at r_0 for being ejected at $t > \tau_D$ of the type $p(r_0) = \Theta(r_0 - R_0 + \Delta R)$ where $\Theta(x)$ is the Heaviside step function.

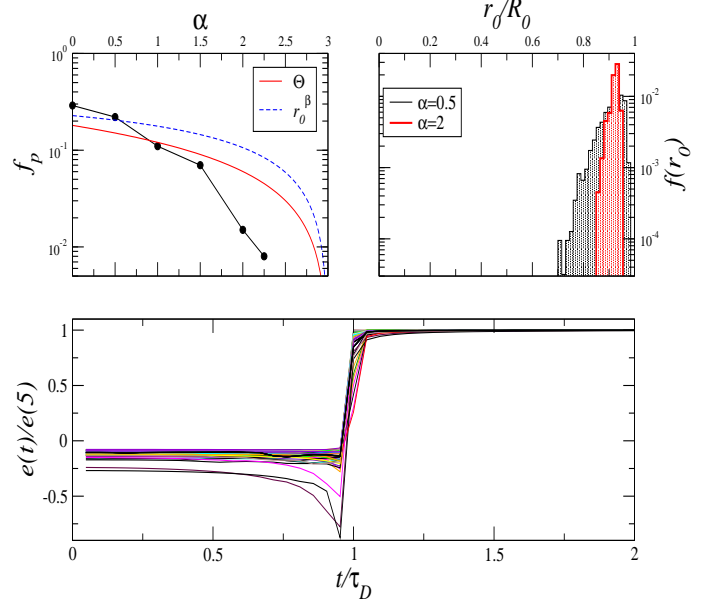


Figure 2. Upper left panel: Number of ejected particles as a function of their initial radial position for $\alpha = 0.5$ and $\alpha = 2$. B Upper right panel: Fraction of the particles with positive energy as a function of α . The dashed line corresponds to a radial probability of ejection described by the Heaviside step function (i.e., $p(r_0) = \Theta(r_0 - R_0 + \Delta R)$ — see Eq.7) while the solid line to a power-law radial probability $p(r_0) \sim r_0^\beta$ with $\beta = 4$ (i.e. Eq.9). Bottom panel: Behaviour of the energy $e_p(t)$ for some of the ejected particles as a function of time, normalised to the energy at $t = 5\tau_D$ and for $\alpha = 0$.

Even in this case the agreement is very rough: however the assumption that $p(r_0)$ has the same exponent for all values of α is probably too strong. Indeed, as mentioned above, the physical mechanism of ejection is due to a complex interplay between the fluctuations present in the distribution and the finite size of the system.

3.3 Energy exchange

It is interesting to consider how individual particles gain energy as they pass through the core. In Fig.2 (bottom panel) it is plotted the behaviour of the energy $e_p(t)$ for some of the particles that will be ejected after the collapse as a function of time, normalised to the energy at late times (i.e. $t = 5\tau_D$) and in the case $\alpha = 0$. One may note that there is a single abrupt change of the energy at $t \approx \tau_D$, a fact that shows that particles are being accelerated by large scale changes of the mean field potential, instead of getting rapid kicks from encounters with individual particles.

A statistical manner to monitor how particles energy changes during time consists in measuring the quantity (Sylos Labini 2012)

$$\langle \Delta^2(t) \rangle = \frac{1}{N(N-1)} \frac{\sum_{i,j=1}^N i \neq j (e_p^i(t) - e_p^j(t))^2}{\langle e(t) \rangle^2} \quad (10)$$

where $e_p^i(t)$ the average energy per particle is defined as

$$\langle e(t) \rangle = \frac{\sum_{i=1}^{N_t} e_p^i(t)}{N}. \quad (11)$$

Fig.1 (bottom right panel) shows the behaviour of $\Delta_N^2(t) = \langle \Delta^2(t) \rangle - \langle \Delta^2(0) \rangle$ in the various simulations: this changes with time when particles exchange energy, i.e. when the particle normalised energy distribution changes.

It is interesting to note that while for $\alpha = 0$ the exchange of energy occurs simultaneously with the strongest phase of the collapse at $t \approx \tau_D$, for $\alpha > 0$ particles exchange energy also for $t < \tau_D$. This occurs because, for $\alpha > 0$ the i^{th} particle, initially located at $r_0^i > r_0^j \gg 0$, arrives at the centre, if it follows its unperturbed trajectory, later than the j^{th} one (see Eq.5). Thus when the i^{th} particle arrives at the centre, inverting its velocity, it moves in a varying potential field generated by all other particles which were initially placed at distance $< r_0^i$. However the exchange of energy, as long as $r_0 < R_0$, is not enough to allow a fraction of the particles to escape from the system. This is because the gain of kinetic energy depends on the deepness of the potential well and thus on the total mass generating it (Joyce, Marcos & Sylos Labini 2009a).

Finally, we have plotted in Fig.3 the average radial velocity at time t of the particles that at later times, i.e. at $5\tau_D$, have positive (+) and negative (-). One may notice that the change in the radial velocity direction occurs sooner for the latter particles than for the former ones. Particles that will be ejected arrive later than all others, having about the same velocity independently on α . Indeed, as they belong to the outer shell, they are attracted by the same gravitational field. For this reason the dynamics of the ejection is the same for different values of α : what changes is, as previously discussed, only the amount of mass and energy that is ejected from the system.

3.4 Density profile

In the case of an initially uniform density profile, i.e. $\alpha = 0$, the radial density profile of the virialized structure formed by bound particles after the collapse was found to have a r^{-4} decay. (Joyce, Marcos & Sylos Labini 2009a; Sylos Labini 2012). For $\alpha > 0$ one may notice (see Fig.4 — upper left panel) that at small radii the different profiles have different slopes which are close to the initial ones (for a value of the radius of order of the force softening length ε the profile seems to flatten, probably due to the fact that the interaction is smoothed) A simple interpretation of this behaviour is the following: particles in the dense core were already very strongly bound at $t = 0$, as the density has a cusp for $\alpha > 0$ by construction; thus the energy exchange during the violent phase of the collapse represents a small perturbation that is not able to alter significantly the inner particles trajectories.

On the other hand for $r/R_0 \approx 1$ all profiles converge to the same shape, i.e. $n(r) \sim r^{-4} \forall \alpha$. We thus conclude that the dynamical mechanism underlying the formation of the r^{-4} should be the same for all α values, i.e. it is related to process giving rise to mass and energy ejection.

A simple way to focus on the properties of the r^{-4} tail is to monitor how this changes during time evolution. Indeed, as mentioned above, in the case $\alpha = 0$, the large scale tail which decays as $n(r) \sim r^{-4}$ is made of particles with almost

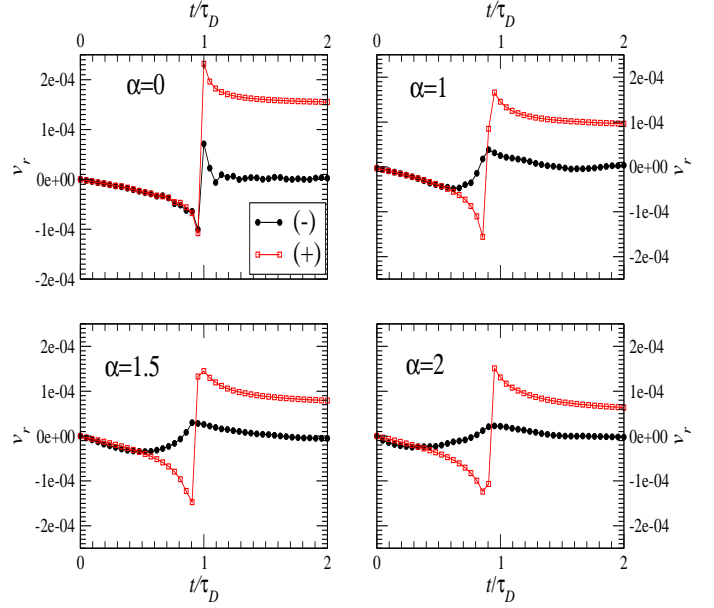


Figure 3. Behaviour of the average radial velocity for particles that at $t = 5\tau_D$ are bound (-) and ejected (+).

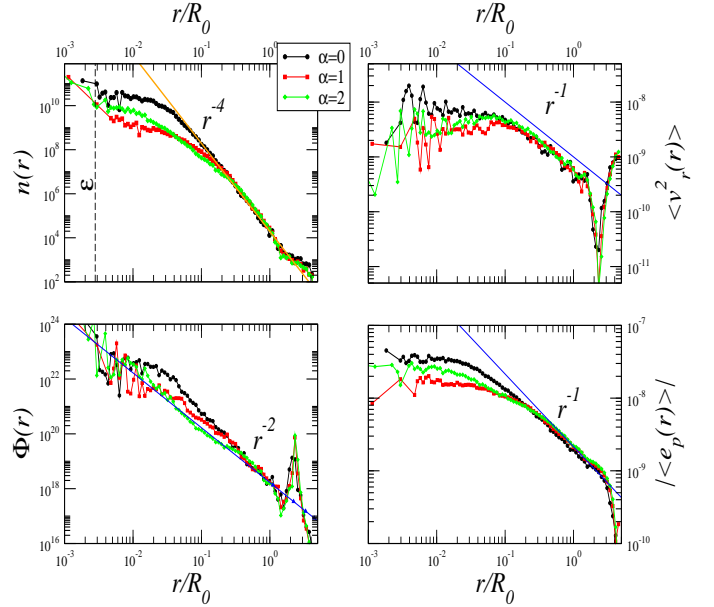


Figure 4. Upper left panel: Density profiles $n(r)$ at $t = 5\tau_D$: the amplitude for $\alpha > 0$ has been arbitrarily normalised to have the same large radii amplitude of $n(r)$ for $\alpha = 0$. Upper right panel: Square value of the radial component of the velocity $\langle v_r^2(r) \rangle$ as a function of the radius at $t = 5\tau_D$ for different values of α . Bottom left panel: Pseudo phase-space density $\Phi(r)$ as a function of the radius at $t = 5\tau_D$ for different values of α : the different curves have been normalised to have same amplitude at large radii as the $\alpha = 0$ case. Bottom right panel: Average energy per particle $\langle e_p(r) \rangle$ (absolute value) as a function of the radius and for different values of α .

zero energy orbiting around the dense core at smaller radii. As time passes these particles may reach larger and larger radii and thus the tail extends to larger and larger radii. This is indeed what is observed not only in the case $\alpha = 0$ but also for $\alpha > 0$. This evidence corroborate the conclusion that the density profile tail properties have the same physical origin for all α values. We will come back on this point in what follows.

3.5 Radial velocity dispersion profile

In Fig.4 (upper right panel) it is shown the mean square value of the radial velocity as a function of the radius $\sigma_r^2(r) = \langle v_r^2(r) \rangle$ at $t = 5\tau_D$ for different values of α . One may note that the different curves are almost indistinguishable and that at large radii, i.e. $r/R_0 > 0.1$, they show an approximated Keplerian $\sigma_r^2(r) \sim r^{-1}$ behaviour.

The time evolution of $\langle v_r^2(r) \rangle$ is again very similar for different values of α and compatible with the physical model presented in Sylos Labini (2012): a few particles with almost zero energy continue to increase their distance from the structure core, remaining however bound. Note that, at a given time, the break of the r^{-1} behaviour is found at the same radii for different values of the α : this reflects the fact that particles belonging to the tail not only obey to the same equation of motions but also are subjected to the gravitational effect of approximately the same core mass.

3.6 Pseudo phase-space density

The behaviour pseudo phase-space density $\Phi(r) = n(r)/\sigma_r^3(r)$ (see Fig.4 — bottom left panel) is a combination of the density and radial velocity dispersion profiles. In agreement with the previous results, at large enough radii it shows the same behaviour independently on α ; indeed, a fit with a function of the type $\Phi(r) \sim \frac{r^{3/2}}{r^4} \sim r^{-5/2}$ describes only the large scale tail. Finally we note that, as for the radial velocity dispersion, at a given time, the break of the $r^{-5/2}$ tail is found at the same scale for different values of α (in this, at $t = 5\tau_D$, there is a bump at $r/R_0 \approx 3$).

3.7 Energy distribution

The distribution of particles total energy at $t \approx 5\tau_D$, i.e. when the virialized structure is already formed, is shown in Fig.5 (left panel). One may note that the larger is α the smaller is the fraction of particles with positive energy, a result clearly in agreement with the ejection mechanism discussed in Sect.3.2.

The average energy of a particle with radial distance r from the structure centre is displayed in Fig.4 (bottom right panel). At large radii, i.e. $r > 1/10R_0$, the energy displays a r^{-1} behaviour, in agreement with the fact that the gravitational potential energy is dominated by the inner core and thus that the velocity dispersion presents a Keplerian decay. On the other hand, at small radii, the different density profile give rise to slightly different potential and kinetic energy profiles.

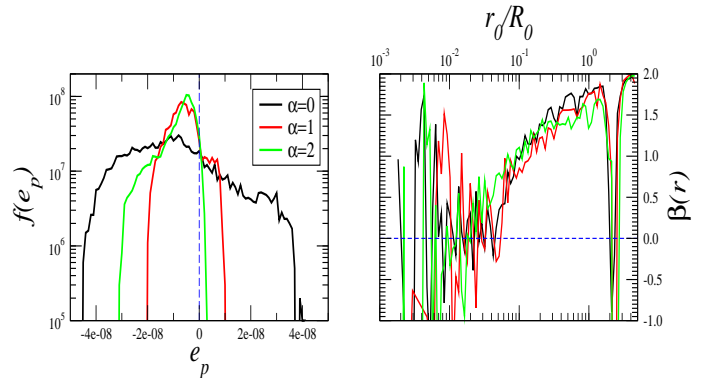


Figure 5. Left panel: Particle total energy distribution for different values of α Right Panel: Velocity anisotropy at $t = 5\tau_D$. When $\beta(r) > 0$ the velocity dispersion is dominated by its radial component.

3.8 Velocity anisotropy

Fig.5 shows the behaviour, in the different simulations, of the velocity anisotropy parameter defined as

$$\beta(r) = 2 - \frac{v_t(r)^2}{v_r(r)^2}, \quad (12)$$

where $v_t(r)/v_r(t)$ is the velocity in the transversal/radial direction. In the outer regions of the virialized structure where the density scales as $n(r) \sim r^{-4}$, radial orbits dominate the motion, as it was already noticed by van Albada (1982); Trenti, Bertin & van Albada (2005); Sylos Labini (2012) for the $\alpha = 0$ case. It is interesting to note that not only the behaviour of $\beta(r)$ is essentially the same for different values of α , but also its amplitude. This, together with the evidences already discussed from the radial velocity dispersion and its time dependence, confirms the fact that the particle dynamics in the large scale tail is the same for all values of α considered.

3.9 The case of a nonzero initial velocity dispersion

For an initially uniform cloud (i.e., $\alpha = 0$) and for warm enough initial velocity dispersion ejection of mass and energy does not occur anymore. In Sylos Labini (2012) we found that the critical value of the initial virial ratio was $b_0^c \approx -1/2$: for $b_0 > b_0^c$ ejection occurs and for $b_0 < b_0^c$ it does not occur anymore. The value of b_0^c is approximate as it was conjectured to depend on the number of points N used in the simulation. The reason for not having ejection anymore is due to the fact that an high enough velocity dispersion cause shell crossing well before the collapse time τ_D . Such a shell crossing erase the temporal lag of the outer shell, thus avoiding that particles initially placed at the outer boundaries of the system arrive later, then moving in a rapidly time varying gravitational field.

A similar mechanism should be working also for $\alpha > 0$. For each value of α and for each N one should be able to find a critical value of the initial virial ratio, i.e. $b_0^c =$

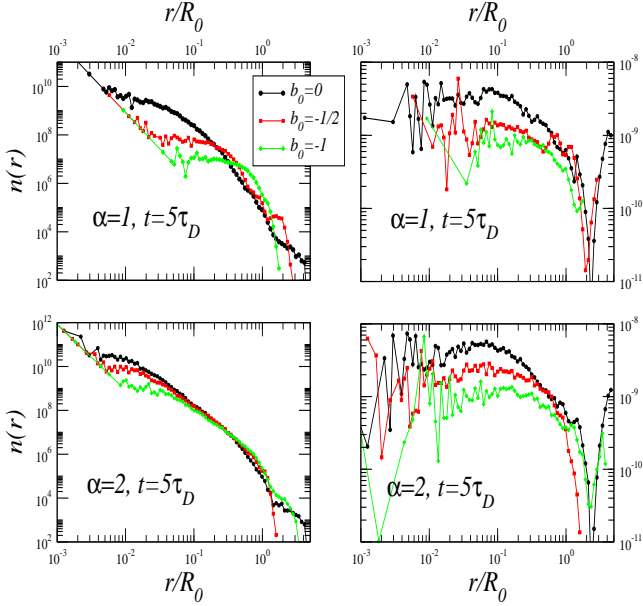


Figure 6. Density profile and velocity dispersion for $\alpha = 1$ (upper panels) and $\alpha = 2$ (bottom panels) and $b_0 = 0, -1/2, -1$ at $t = 5\tau_D$.

$b_0^c(N; \alpha)$. Here we have limited our study to $b_0 = -1/2, -1$ and $\alpha = 1, 2$ for which we have not found mass and energy ejection. Instead of determining the precise value of b_0^c we are interested here in the shape of the density and velocity profiles when ejection does not occur.

In this case the collapse is more gentle, and the virial ratio shows a series of damped oscillations which drive the system toward the quasi-equilibrium state. In Fig.6 we show respectively the density profile, velocity dispersion and pseudo phase-space density for $\alpha = 1, 2$ and $b_0 = 0, -1/2, -1$. One may note that (i) the smaller is b_0 and the smaller the difference between the input and output density profile. (ii) For different values of b_0 there is a difference in the behaviour of all density and velocity profiles, a fact that points toward an important role of the initial conditions. (iii) The case $\alpha = 2$ presents the smaller change in the density profile $n(r)$ between the initial and final condition: the larger is α and the deeper the potential well at small scales and thus the smaller the perturbation introduced by a given amount of kinetic energy. We thus conclude that when the collapse is violent, for the effect on an initial velocity dispersion, there is a clear dependence of the virialized structure properties on the initial conditions.

4 RELAXATION OF MORE COMPLEX DENSITY PROFILES

In this section we have considered an initially perfectly cold cloud of self-gravitating particles, whose profile is described by: (i) the Plummer sphere

$$n(r) = \frac{A}{\left(1 + \frac{r^2}{r_s^2}\right)^{\frac{5}{2}}}, \quad (13)$$

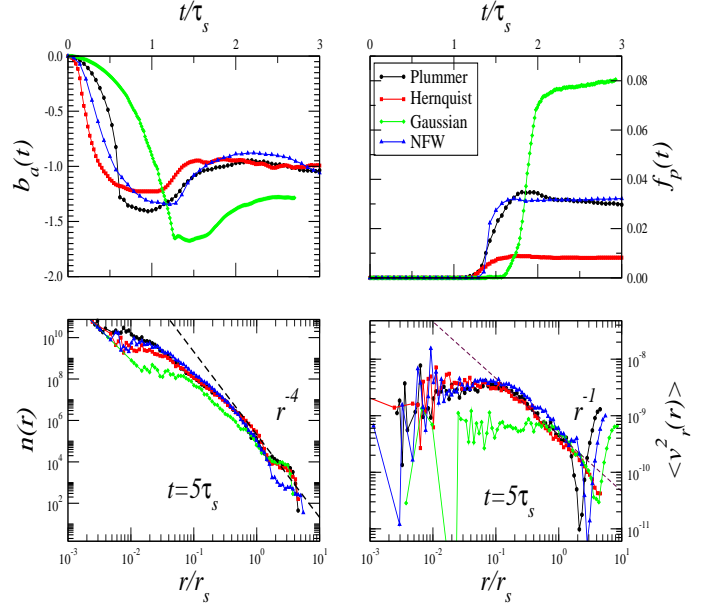


Figure 7. Upper left panel: Virial ratio of all particles. Upper right panel: Fraction of particles with positive energy. Bottom left panel: density profiles $n(r)$ at $t = 5\tau_D$. Bottom right panel: radial velocity dispersion $\langle v_r^2(r) \rangle$ at $t = 5\tau_D$.

(ii) the Hernquist profile ($\gamma = 3$), (iii) the NFW profile ($\gamma = 2$)

$$n(r) = \frac{A}{r \left(1 + \frac{r}{r_s}\right)^\gamma}, \quad (14)$$

and the (iv) Gaussian profile

$$n(r) = A \exp\left(-\left(\frac{r}{r_s}\right)^2\right), \quad (15)$$

where in Eqs.13-15 A and r_s are two constants that are fixed by the number of points N_p initially belonging to the cloud and by the requirement that the radius enclosing half of the mass is the same for all profiles, so that the collapse time is about the same in the different cases.

Results are shown in Fig.7: we have normalised the time to the characteristic time τ_s for collapse for each density profile and the radius to r_s defined in Eqs.13-15. One may note that there are similarities with the behaviours found in Figs.1-4. In particular in all cases it is observed ejection of a fraction of the particles and the formation of a $n(r) \sim r^{-4}$ density profile and a radial velocity dispersion decaying as r^{-1} . Qualitatively the dynamics is thus similar to the case discussed in the previous section.

5 DISCUSSION AND CONCLUSIONS

The collapse of an isolated spherical cloud of self-gravitating particles represents a paradigmatic example of the dynamics giving rise, through a global relaxation process, to a virialized structure in a quasi-equilibrium state, i.e. a state that

has a life-time that diverges with the number of system particles and that is far from thermodynamical equilibrium. If the collapse is violent enough part of the initial mass and energy of the cloud is ejected in the form of free particles. This ejection occurs, for the case of an initially uniform cloud, when the initial velocity dispersion is small enough (Sylos Labini 2012). In this case some non-trivial density and velocity profiles have been observed: (i) the radial density decays as $n(r) \sim r^{-4}$ at large enough radii, (ii) the radial velocity dispersion decays as $\sigma_r^2 \sim r^{-1}$ and thus (iii) the pseudo phase-space density decays as $n(r)/\sigma_r^3(r) \sim r^{-5/2}$ (Sylos Labini 2012). All these behaviors can be understood in the framework of a simple dynamical model in which the bound particles that have the largest energies, belong to the tail of the profile and are orbiting in a central gravitational potential generated by the inner dense core (Sylos Labini 2012).

The problem that we have considered in this paper concerns whether the same density and velocity profiles are observed when the initial conditions are not represented by a uniform cloud of particles. In particular, we have firstly considered an initial density profile of the type $n(r) \sim r^{-\alpha}$ with $0 \leq \alpha < 3$. When the initial velocity dispersion is zero, the situation for $\alpha > 0$ is similar to the uniform case, i.e. $\alpha = 0$, in various aspects. During the collapse phase a fraction of the particles gain enough kinetic energy to escape from the system, i.e. there is ejection of mass and energy. The virialized structure formed after the collapse presents, at large enough radii, the same behaviors (i)-(iii) discussed above for the initially uniform cloud. In addition, radial orbits dominate the motion of particles in the density profile tail in all cases. The time evolution of these quantities shows that the underlying dynamics determining the large radii properties of the virialized structures is identical to the $\alpha = 0$ case. These common features are thus generated by the dynamical mechanism acting during the collapse, and responsible of the mass and energy ejection. For this reason they are independent on the initial properties of the self-gravitating cloud.

On the other hand, when the initial velocity dispersion is high enough, we find that there is no ejection of mass and energy so that the density and velocity profiles do not present any power-law behaviour at large radii. In this case the collapse is more gentle and consists in a few oscillations that drive the system to a quasi-equilibrium configuration and the virialized structure displays features that depend on the initial conditions.

In addition, we have considered other initial density profiles which are not scale-free, as the Plummer, the Hernquist, the NFW and the Gaussian profile. In all these cases we found that, when the initial velocity dispersion is set to zero, the density profiles converges, for large enough radii, at the same behaviors (i)-(iii) discussed above. These results are in agreement with Visbal, Loeb & Hernquist (2012) who have recently found that a Plummer sphere, originally at rest, collapses, in simulations where non-radial motions are both present or suppressed, forming a virialized state with a r^{-4} tail at large radii. Note that a simple explanation for the formation of the r^{-4} was proposed by White (1987); Jaffe (1987); in Sylos Labini (2012) we introduced a more detailed model of particle dynamics, which considers as well the behaviour of the bound particles with almost zero total

energy, and a series of analyses that corroborate the hypothesis that particle with very small binding energies form the r^{-4} tail.

We thus conclude that when a cloud undergoes a violent collapse, i.e. when part of its initial particles gain energy during the collapse to eventually escape as free ones, it reaches a virialized quasi-equilibrium configuration that displays properties which are formed by the dynamical relaxation mechanism. In particular, these features characterise the tail of the density and radial velocity dispersion profiles and they are related to the behaviour of those bound particles which were initially in the outer shells of the distributions.

Instead, strongly bound particles, i.e. those in the central dense core, have properties which depend on the initial conditions. These are the particles which already initially were strongly bound, given the cusp of the density profile: for this reason the energy exchange during the violent phase of the collapse represents a small perturbation that is not able to alter significantly their trajectories.

As a final remark we note that the systems considered here, although pose a series of interesting theoretical questions, differ for many important aspects not only from real systems but also from structures formed in cosmological N-body simulations. In particular, a more detailed study of the modification of the isolated system dynamics due to space expansion, continuous mass accretion, merging with macro objects and tidal interactions with background structures and a careful analysis of numerical and finite size issues Joyce & Sylos Labini (2012) is necessary to clarify the relation between the simple self-gravitating clouds considered in this paper and halos formed in cosmological simulations.

I thank Michael Joyce for useful discussions and comments, Roberto Ammendola and Nazario Tantalò for the valuable assistance in the use of the Fermi supercomputer where the simulations have been performed.

REFERENCES

- Aarseth S., Lin D., Papaloizou J., 1988, *Astrophys. J.*, 324, 288
- Boily C., Athanassoula E., 2006, *Mon. Not. R. Astr. Soc.*, 369, 608
- Hénon M., 1964, *Ann. Astrophys.*, 27, 1
- Hernquist L., 1990, *Astrophys. J.*, 356, 359
- Jaffe, W., 1987, *IAU Symposium*, Vol. 127, *Structure and Dynamics of Elliptical Galaxies*, ed. P. T. de Zeeuw & S. D. Tremaine, 511
- Joyce M., Marcos B., Sylos Labini F., 2009, *Mon. Not. R. Astr. Soc.*, 397, 775
- Joyce M., Marcos B., Sylos Labini F., 2009, *Journal of Statistical Mechanics*, P04019
- Joyce M. and Sylos Labini F., 2012 [arXiv:1210.1140](https://arxiv.org/abs/1210.1140)
- Navarro J. F., Frenk C. S., White S. D. M., 1997, *Astrophys. J.*, 490, 493
- Springel V., Yoshida N., White S. D. M., 2001, *New Astronomy*, 6, 79
- Springel V., 2005, *Mon. Not. R. Astr. Soc.*, 364, 1105
- Sylos Labini F., 2012, *Mon. Not. R. Astr. Soc.* 423, 1610
- Theis Ch. & Spurzem R., 1999 *Astron. Astrophys.*, 341, 361

- Trenti M., Bertin G. & van Albada T.S. 2005, *Astron.Astrophys.*, 433, 57
van Albada T., 1982, *Mon.Not.R.Astr.Soc.*, 201, 939
Visbal E., Loeb A. & Hernquist L., 2012, [arXiv:1206.5852](https://arxiv.org/abs/1206.5852)
White, S.D., S. D. M. 1987, in *IAU Symposium*, Vol. 127, *Structure and Dynamics of Elliptical Galaxies*, ed. P. T. de Zeeuw & S. D. Tremaine, 339